materials

MDPI

Article

Multiple Intermolecular Interaction to Improve the Abrasion Resistance and Wet Skid Resistance of Eucommia Ulmoides Gum/Styrene Butadiene Rubber Composite

Mingyang Li, Kuiye Wang and Yuzhu Xiong *

Department of Polymer Materials and Engineering, College of Materials and Metallurgy, Guizhou University, Guiyang 550025, China; lmy897817576@126.com (M.L.); 15705427406@163.com (K.W.)
* Correspondence: yzxiong@gzu.edu.cn

Abstract: A rubber composite was prepared by using methyltriethoxysilane (MTES) to modify silica (SiO_2) and epoxidized eucommia ulmoides gum (EEUG) as rubber additives to endow silica with excellent dispersion and interfacial compatibility under the action of processing shear. The results showed that compared with the unmodified silica-reinforced rubber composite (SiO_2/EUG/SBR), the bound rubber content of MTES-SiO_2/EEUG/EUG/SBR was increased by 184%, and its tensile strength, modulus at 100% strain, modulus at 300% strain, and tear strength increased by 42.1%, 88.5%, 130.8%, and 39.9%, respectively. The Akron abrasion volume of the MTES-SiO_2/EEUG/EUG/SBR composite decreased by 50.9%, and the wet friction coefficient increased by 43.2%. The wear resistance and wet skid resistance of the rubber composite were significantly improved.

Keywords: silica; synergetic modification; compound material; wear resistance; wet skid resistance

Citation: Li, M.; Wang, K.; Xiong, Y. Multiple Intermolecular Interaction to Improve the Abrasion Resistance and Wet Skid Resistance of Eucommia Ulmoides Gum/Styrene Butadiene Rubber Composite. *Materials* **2021**, *14*, 5246. https://doi.org/10.3390/ma14185246

Academic Editor: Lucjan Chmielarz

Received: 16 July 2021
Accepted: 6 September 2021
Published: 12 September 2021

1. Introduction

Silica is an important reinforcing material in industrial production [1]. In the 1940s, the production of silica was industrialized. Today, in addition to being used in food, toothpaste, ink, and pesticides, silica is also widely used in the rubber industry as a reinforcement [2,3]. In the tire industry, adding silica can reduce the heating and rolling resistance of the tread rubber [4,5], and improve the wet skid resistance and abrasion resistance of the tire [6–10]. Therefore, silica is a tire reinforcing filler with great development prospects [11–15]. However, the dispersibility of silica in the composite material is rather poor and the agglomeration is serious because of the large quantities of silanol groups on the surface of silica and high surface energy [16–19]. Therefore, improving the dispersion [20–24] of silica in composite materials by pretreatment is a hot research topic [25–29].

The silane coupling agent can react with silanol on the surface of silica to form covalent bonds, reduce the silanol density of the silica surface, and improve the compatibility of silica with the rubber matrix, leading to the improvement in filler dispersion and the performance of the rubber composite [30]. Bertora [31] used the small molecule coupling agent mercaptosilane (KH590) to graft liquid polybutadiene on the surface of silica and add it to the SBR, where the surface hydrophobicity of the rubber increased, the degree of filler aggregation decreased, and the dispersibility was improved. Dong [32] studied the effect of modified silica on the vulcanization kinetics of natural rubber (NR)/styrene butadiene rubber (SBR) blends. It was found that the vulcanization rates of NR and SBR phases in blends filled with KH560-modified silica were almost the same, showing a better co-vulcanization effect. In addition, compared with untreated silica, modified silica could be uniformly dispersed and improved the mechanical strength of the rubber blend [33,34].

The polar groups in polymers can interact with silica by forming hydrogen bonds or covalent bonds. Thus, polymers with polar groups have been used as alternatives to silane couplings [35,36]. Eucommia ulmoides gum (EUG) is a natural rubber whose main

component is trans-polyisoprene, which is an isomer of natural rubber. Epoxidation is a popular chemical modification method for polydiolefin rubbers. The epoxidized eucommia ulmoides gum (EEUG) shows a higher polarity than original EUG because of the epoxy groups in its structure [37]. EEUG has been used as a compatibilizer in filled systems. Wang [38] modified silica with a macromolecular modifier (EEUG) and added it to SBR. The dispersion of modified silica was better, the wear resistance of the compound was improved, and the wear volume decreased from 0.192 cm^3 to 0.179 cm^3.

In this work, we first modified the silica with a small molecule coupling agent methyltriethoxysilane (MTES), and added it to the rubber matrix together with EEUG to prepare the composite material. The schematic diagram of the synergistic effect of MTES and EEUG on silica is presented in Figure 1. The small-molecule coupling agent (MTES) reacted with the silanol groups on the surface of SiO_2 to form a covalent bond, which reduced the surface activity of SiO_2 and reduced its agglomeration tendency. The epoxy group on the EEUG macromolecule can form hydrogen bonds or undergo a ring-opening reaction with the silanol groups on the surface of silica to form a covalent bond; this anchors part of the silica to the EEUG molecular chain, which increases the silica and interfacial compatibility of the rubber matrix. During processing, the shear flow of EEUG molecular chains drives better dispersion of silica to obtain rubber composites with excellent properties.

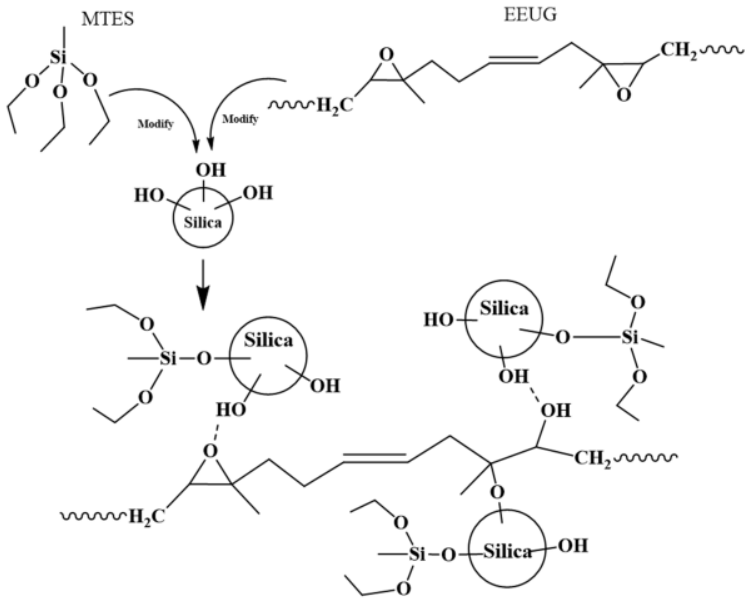

Figure 1. Schematic diagram of the synergistic effect of methyltriethoxysilane (MTES) and epoxidized eucommia ulmoides gum (EEUG) on silica.

2. Materials and Methods

2.1. Materials

Eucommia ulmoides gum (EUG) was purchased from Shandong Qingzhou Beilong Company (Weifang, China); SBR was purchased from Lanzhou Petrochemical Co. Ltd. (Lanzhou, China); silica (SiO_2) was purchased from Changzhou Lehuan Chemical Co. Ltd. (Changzhou, China); methyltriethoxysilane (MTES), sodium dodecylbenzene sulfonate, hydrogen peroxide (H_2O_2), and sodium bicarbonate ($NaHCO_3$) were purchased from Shanghai Aladdin Biochemical Technology Co. Ltd. (Shanghai, China); zinc oxide (ZnO), stearic acid (SA), accelerator (DM), antioxidant 4020, and sulfur (S) were obtained from Guizhou Tire Factory (China). Petroleum ether and absolute ethanol were purchased from Chongqing Chuandong Chemical Co. Ltd. (Chongqing, China). Formic acid (HCOOH) was purchased from Tianjin Fuyu Fine Chinese Industrial Co. Ltd. (Tianjin, China). Deionized water was made in-house.

2.2. Preparation of EEUG

EUG (50 g) was added to a 2000 mL beaker, followed by the addition of 900 mL petroleum ether. Then, the beaker was placed in a 45 °C constant-temperature water bath, and mechanically stirred until the gum was completely dissolved. Second, 300 mL deionized water and 2.5 g sodium dodecylbenzene sulfonate were added, and stirring was continued to form a stable emulsion. Then, quantitative HCOOH was added, and the corresponding amount of H_2O_2 was slowly added (the molar ratio of double bonds, HCOOH, and H_2O_2 was 1:0.8:2). The reaction lasted for 1 h at 45 °C under mechanical stirring. After epoxidation, hot saturated $NaHCO_3$ solution was added to the beaker to adjust the pH of the EEUG solution to 7. Then, absolute ethanol was added to precipitate EEUG. The product was dried to constant weight at room temperature to obtain 49.25 g of the desired EEUG. A small amount of EEUG was mixed with unmodified SiO_2 (denoted as EEUG-SiO_2) for infrared spectroscopy (Nexus 6700, Thermo Scientific, MA, USA) and XPS spectrum analysis (Thermo Fisher K-Alpha, Shenzhen Junhuiteng Technology Co. Ltd., Shenzhen, China).

2.3. MTES Modified SiO_2

A tray of SiO_2 was placed in a vacuum oven at 80 °C for 12 h to remove moisture. Dried SiO_2 (30 g) was poured into a three-necked flask, and then 450 mL absolute ethanol was added, with ultrasonic treatment for 35 min. MTES (6 g) was poured into a beaker, and then 60 mL absolute ethanol was added, and ultrasonic treatment was performed to form an emulsion. A three-necked flask containing SiO_2 was placed in a 60 °C water bath, mechanically stirred, and heated at reflux. The pre-emulsified MTES was then added dropwise. The product was taken out after 2 h, aged for 1 h, and washed three times with absolute ethanol. After suction filtration, it was dried in a vacuum oven at 80 °C to obtain MTES-modified SiO_2 (denoted as MTES-SiO_2). A small amount of EEUG was mixed with MTES-SiO_2 (denoted as EEUG-MTES-SiO_2) for infrared spectroscopy and XPS spectrum analysis.

2.4. Preparation of Rubber Composites

According to the ratios listed in Table 1, SBR, EUG, EEUG, SiO_2, and MTES-SiO_2 were mixed in three stages in an internal mixer (XSM-05, Shanghai Kechuang Rubber Machinery Equipment Co. Ltd., Shanghai, China), each with a temperature of 125 °C, 130 °C, and 135 °C, a rotor speed of 80 rpm, and a mixing time of 7 min. After the mixture was cooled, the roller temperature of the open mill (Φ160 × 320, Dongguan Changfeng Rubber Machinery Co. Ltd., Dongguan, China) was adjusted to about 70 °C. The prepared mixture was placed on the open mill for 3 min and passed twice. It was used to wrap the roller, and then ZnO, SA, antioxidant 4020, DM, and S were added sequentially according to the ratio in Table 1. After all the ingredients were added, it was thinned up to five to seven times, and then the roller distance was evenly and slowly adjusted to the left and right, so that the mixture was discharged with a thickness of about two millimeters. The obtained sheet-like mixture was laid flat at room temperature and a humidity of 40–50% for 24 h to eliminate internal stress. Then, a part of the mixture was used to make samples by air pressure by putting round cake-shaped test samples in a rotorless auto-vulcanization instrument (MD-3000A, Taiwan High-Speed Rail Technology Co. Ltd., Taichung City, Taiwan) to determine the positive vulcanization time. Then, the mixture was cut into a size suitable for the vulcanization mold. It was put into a flat vulcanizer (XLB-25t, Jiangdu Mingzhu Experimental Machinery Factory, Yangzhou, China) at a vulcanization temperature of 150 °C. The vulcanization time was based on the positive vulcanization time obtained by the test. The prepared rubber composite material was laid flat at room temperature and a humidity of 40–50% for 24 h to eliminate internal stress.

Table 1. Rubber composite formula (phr).

Sample	#1	#2	#3	#4
SBR	70	70	70	70
EUG	30	30	24	24
EEUG	0	0	6	6
SiO_2	30	0	30	0
MTES-SiO_2	0	30	0	30
ZnO	5	5	5	5
SA	4	4	4	4
DM	2	2	2	2
Antioxidant 4020	1	1	1	1
S	2.5	2.5	2.5	2.5

The formulation of the rubber composite is shown in Table 1, where #1 is a composite prepared from unmodified SiO_2, EUG, and SBR, denoted as SiO_2/EUG/SBR; #2 is a composite prepared from MEST-SiO_2, EUG, and SBR, denoted as MEST-SiO_2/ EUG/SBR; #3 is a composite prepared from unmodified SiO_2, EEUG, EUG, and SBR, denoted as SiO_2/EEUG/EUG/SBR; and #4 is a composite prepared from MTES-SiO_2, EEUG, EUG, and SBR, denoted as MTES-SiO_2/EEUG/EUG/SBR.

2.5. Testing and Characterization

2.5.1. Fourier-Transform Infrared (FTIR) Spectroscopy

Unmodified SiO_2, MTES, EEUG, EEUG-SiO_2, MTES-SiO_2, and EEUG-MTES-SiO_2 were characterized with a Fourier-transform infrared spectrometer (Nexus 6700, Thermo Scientific, MA, USA), with a scanning wavenumber range of 400–4000 cm^{-1}.

2.5.2. X-ray Photoelectron Spectroscopy (XPS)

XPS spectra of SiO_2, MTES-SiO_2, EEUG-SiO_2, and EEUG-MTES-SiO_2 were recorded by using an X-ray photoelectron spectrometer (Thermo Fisher K-Alpha, Shenzhen Junhuiteng Technology Co. Ltd., Shenzhen, China). Samples were analyzed under vacuum ($p < 10^{-8}$ mbar) with a pass energy of 150 eV (survey scans) or 50 eV (high-resolution scans). All peaks were calibrated with C1s peak binding energy at 284.8 eV for adventitious carbon.

2.5.3. Determination of Bonding Rubber

Rubber (0.5 g) was crushed with scissors into small pellets, wrapped in copper mesh, and immersed in 60 mL of toluene for three days. The toluene was refreshed every 24 h. After that, it was immersed in 600 mL of acetone for 24 h. The toluene was removed, and the remaining rubber was placed in an oven at 60 °C for drying until its mass did not change; each sample was tested for three times. The bonding rubber content w was calculated as follows:

$$w = \frac{w_1 - (w_2 - w_3)}{w_1} \times 100\% \quad (1)$$

where w_1 is the rubber mass of the sample; w_2 is the mass of rubber and copper mesh; and w_3 is the mass of the remaining rubber and copper mesh after drying to a constant weight.

2.5.4. Curing Characteristics

A rotorless vulcanizer (MD-3000A, Taiwan High-Speed Rail Technology Co. Ltd.) was used to test the curing characteristics of the rubber composite. The test temperature was 150 °C, the test time was 40 min, the rotation angle was 0.5°, the stabilization time was 1 s, and the stability range was 0.50 °C; each sample was tested twice.2.5.5. Rubber Processing Analyzer

A rubber processing analyzer (RPA2000, Alpha, Technologies, Hudson, OH, USA) was used to determine the storage modulus G' and loss factor $tan\delta$ of the rubber composite, with a strain sweep range of 0.7–400%, temperature of 60 °C, and frequency of 1 Hz.

2.5.5. Mechanical Performance Testing

According to GB/T528-1998, the rubber was prepared into dumbbell-shaped specimens and analyzed with a universal material testing machine (Inspeakt Table 10 kN, Germany Huibo Material Testing Company, Beijing, China). The tensile rate was 500 mm/min, and each sample was tested five times.

2.5.6. Akron Abrasion Test

A special mold was used to prepare the rubber material into a strip sample, which was then glued to a rubber wheel, and allowed to stand for 8 h. Then, a testing instrument (ZB-201, Jiangsu Zhengrui Taibang Electronic Technology Co. Ltd., Yangzhou, China) was used to test the Akron abrasion volume (V) using a test angle of 15°. First, the sample was pre-ground 600 revolutions, and the fallen rubber crumbs were collected and weighed, accurate to 0.001 g, and the weight was recorded as m_1. The pre-ground sample was ground for another 3416 revolutions, then the fallen rubber crumbs were collected and weighed again, and the weight was recorded as m_2. The density (ρ) of the sample was tested according to GB/T533; each sample was tested three times. The Akron abrasion volume V was calculated using the following equation:

$$V = \frac{m_1 - m_2}{\rho} \quad (2)$$

2.5.7. SEM Analysis

Scanning electron microscope (SEM, JSM-7500F, JEOL Ltd., Beijing, China) was used to observe the tensile fracture surface morphology of the composite and the wear surface morphology after Akron abrasion tests.

2.5.8. Wet Sliding Friction Test

A pendulum friction coefficient tester (BM-III) was used to test the friction coefficient of the rubber composite under wet and slippery conditions. The sliding path was 126 mm, the test temperature of the rubber compound was 25 °C, and the humidity was between 45–55%. Water was sprayed on the glass surface to simulate a wet road. Five rubber sliders were prepared for each composite, and water was sprayed on the glass surface again before each test [9].

3. Results

3.1. FTIR Analysis of the Interaction between SiO_2 and Enhancer

Figure 2 shows the FTIR spectra of unmodified SiO_2, MTES-SiO_2, EEUG-SiO_2, EEUG-MTES-SiO_2, and EEUG. The FTIR spectrum of unmodified SiO_2 contained peaks for the asymmetric stretching vibration of Si–OH at 3436 cm^{-1}, the asymmetric stretching vibration of Si–O–Si and the symmetric stretching vibration peak of Si–O at 1104 cm^{-1} and 800 cm^{-1} [5,36]. In the infrared spectrum of MTES, the peak at 780 cm^{-1} assigns to the bending vibration of Si–C, the peaks at 957 cm^{-1}, 1412 cm^{-1}, and 2978 cm^{-1} corresponded to the characteristic peak of Si–O–CH_2–, the absorption peak of C–H in methyl group, and the stretching vibration peak of –CH_3 [39,40]. In the infrared spectrum of EEUG, the peaks at 2963 cm^{-1}, 2925 cm^{-1}, and 2855 cm^{-1} corresponded to the asymmetric stretching vibration of methyl groups, asymmetric stretching vibration, and symmetric stretching vibration of methylene groups, respectively. The peak at 1250 cm^{-1} is the symmetrical stretching vibration of epoxy group [36]. Comparing the spectra of SiO_2 and MTES-SiO_2, a new stretching vibration peak of -CH_3 appeared at 2978 cm^{-1} [39], indicating that MTES was successfully grafted onto SiO_2. In the spectra of unmodified SiO_2, EEUG, and EEUG-SiO_2, it can be seen that compared with unmodified SiO_2, the EEUG-SiO_2 spectrum contained three characteristic peaks belonging to EEUG at 2963 cm^{-1}, 2925 cm^{-1}, and 2855 cm^{-1}. Compared with the infrared spectrum of EEUG, the epoxy group peak at 1250 cm^{-1} disappeared [37] and the Si–OH peak at 3436 cm^{-1} weakened in the EEUG-SiO_2

spectrum, indicating that the epoxy group of EEUG was opened by the hydroxyl group on the SiO_2 surface. The infrared spectrum of MTES-EEUG-SiO_2 was roughly the same as that of EEUG-SiO_2 because the -CH_3 absorption peak on MTES was incorporated into the -CH_3 absorption peak of EEUG. The above phenomena showed that both the individual modification and synergistic modification of SiO_2 by the small-molecule coupling agent and the macromolecular modifier were successful.

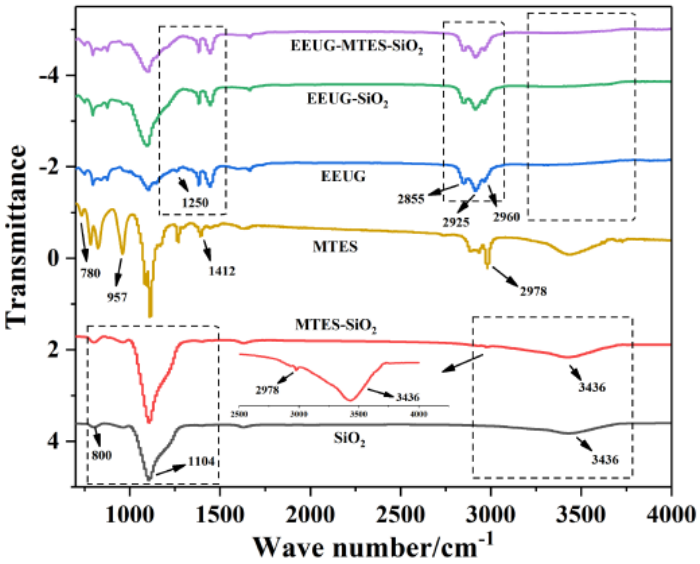

Figure 2. FTIR spectra of EEUG, MTES, SiO_2, and modified SiO_2.

3.2. XPS Analysis of the Interaction between SiO_2 and Enhancer

Figure 3 shows the XPS wide-scan spectra of SiO_2, MTES-SiO_2, EEUG-SiO_2, and EEUG-MTES-SiO_2 and the information of the elemental composition on the surface of the particle are shown in Table 2. It shows that the C1s intensity and element content of C increased and elemental content of Si, O decreased in MTES-SiO_2, EEUG-SiO_2, and EEUG-MTES-SiO_2 compared to SiO_2. This is due to that the reaction of EEUG and MTES on silica's surfaces that results in the reduction of O and Si atoms and the increase in C atoms on the surfaces of the silica particles [41].

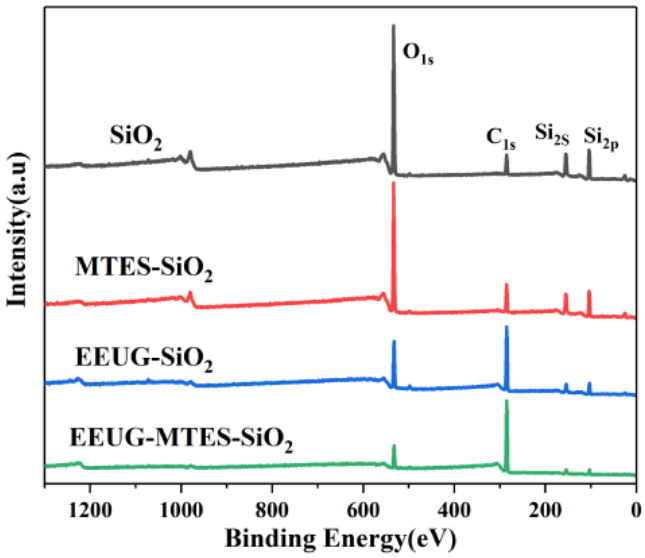

Figure 3. XPS wide-scan spectra of SiO_2, MTES-SiO_2, EEUG-SiO_2, and EEUG-MTES-SiO_2.

Table 2. Comparison of atomic content (at.%) in the XPS spectra of SiO_2, MTES-SiO_2, EEUG-SiO_2, and EEUG-MTES-SiO_2.

Sample	Element Constitution (%)		
	Si	C	O
SiO_2	26.91	18.85	54.24
MTES-SiO_2	24.73	26.51	48.75
EEUG-SiO_2	11.13	66.23	22.64
EEUG-MTES-SiO_2	6.05	82.41	11.54

High-resolution XPS spectra of Si2p for SiO_2, MTES-SiO_2, EEUG-SiO_2, and EEUG-MTES-SiO_2 are shown in Figure 4. It can be seen that the binding energies for Si2p of O–Si–O and Si–O–H groups in SiO_2 were 103.5 eV and 102.8 eV [36], respectively. In MTES-SiO_2, a new peak appeared at 102.1 eV, which stands for the binding energy of Si2p in the Si-C group [42], indicating that MTES is grafted onto SiO_2. In EEUG-SiO_2 and EEUG-MTES-SiO_2, the new peak at 103.65eV is caused by the Si–O–C group [36], implying that the ring opening reaction of epoxy group has taken place. Simultaneously, the binding energy for Si2p of Si–OH shifted to 103eV. This is because a hydrogen bond can form between the epoxy group and silanol, which influences the chemical environment around the Si atom, inducing the shifts of binding energy for Si2p of Si–OH [43,44].

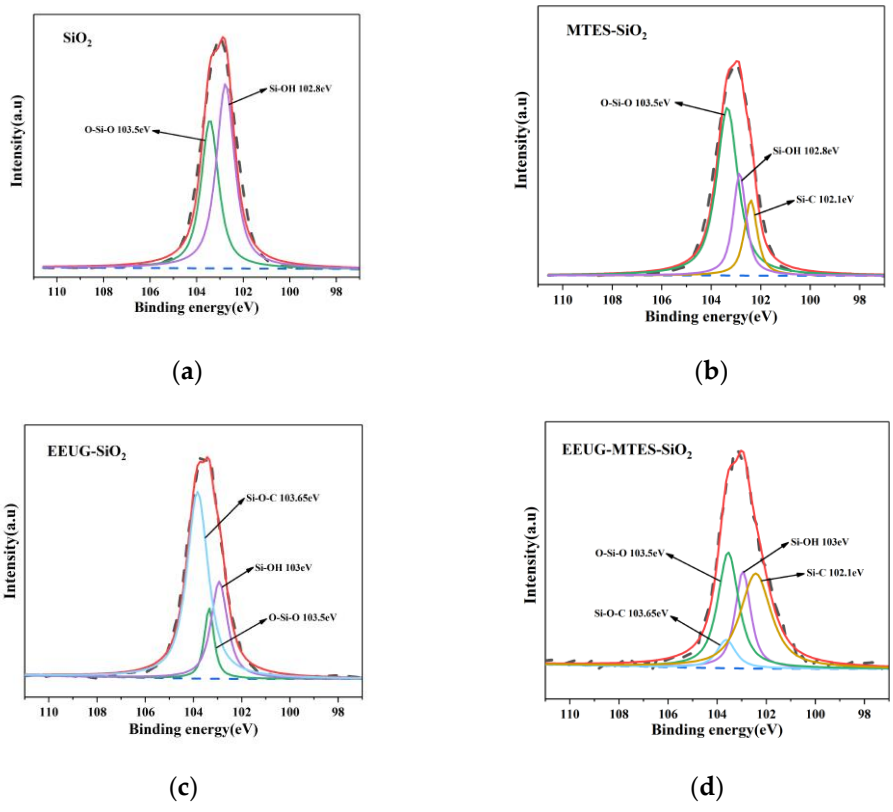

Figure 4. High-resolution XPS spectra of Si2p: (**a**) SiO_2; (**b**) MTES-SiO_2; (**c**) EEUG-SiO_2; (**d**) EEUG-MTES-SiO_2.

3.3. Microstructure of Rubber Composite

Figure 5 shows an SEM image of the tensile fracture surface of the rubber composite. The SEM of SiO_2/EUG/SBR showed that unmodified SiO_2 formed poorly-dispersed large agglomerates in the rubber compound. Obvious phase separation occurred between SiO_2 and the rubber matrix, and the interfacial adhesion between the two was poor [45]. The SEM image of MTES-SiO_2/EUG/SBR showed that after SiO_2 was modified by MTES, MTES

covalently bonded with the silanol groups on SiO_2. Therefore, the steric hindrance effect on the surface of SiO_2 was improved, and the agglomeration of SiO_2 was reduced [46], thus, the particle size of SiO_2 dispersed in the material matrix was reduced and the dispersion was significantly improved. The SEM image of SiO_2/EEUG/EUG/SBR showed that adding EEUG to the matrix also significantly improved the dispersion of SiO_2. The SEM image of MTES-SiO_2/EEUG/EUG/SBR showed that the synergy of MTES and EEUG improved the dispersion and compatibility of SiO_2 with the matrix. The small-molecule coupling agent MTES weakened the degree of SiO_2 aggregation, and the macromolecular modifier EEUG formed hydrogen bonds or bonded with silanol groups. At the same time, SiO_2 bonded to the EEUG molecular chain was better dispersed in the matrix when the rubber molecular chains became entangled and flowed [36,47].

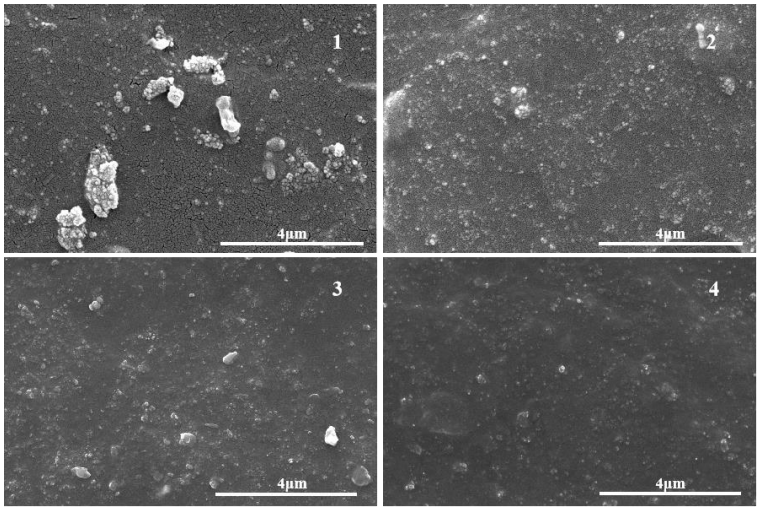

Figure 5. SEM image of the tensile fracture surface of the rubber composite: (1) SiO_2/EUG/SBR; (2) MEST-SiO_2/EUG/SBR; (3) SiO_2/EEUG/EUG/SBR; (4) MTES-SiO_2/EEUG/EUG/SBR.

3.4. Binder Content of Rubber Composite

Figure 6 shows the binder content of rubber composites. Both MTES-modified SiO_2 and the addition of EEUG increased the bound rubber content of the composite. Compared with unmodified SiO_2, the bound rubber content of the composite with both EEUG and MTES-SiO_2 added increased by 184%. Analysis showed that in the rubber composite materials, well-dispersed SiO_2 with interfacial compatibility can increase the degree of interfacial interactions with the rubber matrix; thus, more molecular chains of the rubber matrix will be physically adsorbed on the surface of SiO_2 [48,49]. At the same time, the EEUG molecular chains bonded with SiO_2 will also become physically entangled with the rubber matrix [50], which greatly increases the material's bound rubber content.

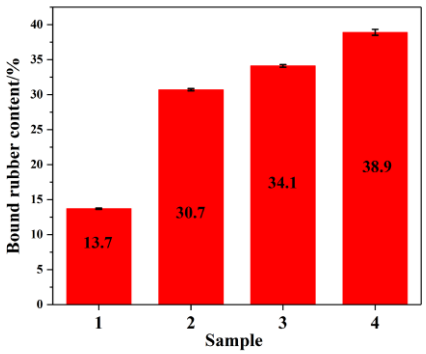

Figure 6. The binder content of rubber composites: (1) SiO_2/EUG/SBR; (2) MEST-SiO_2/EUG/SBR; (3) SiO_2/EEUG/EUG/SBR; (4) MTES-SiO_2/EEUG/EUG/SBR.

3.5. Curing Characteristics of Rubber Composites

The curing characteristics of rubber are important for the manufacture of rubber products. Figure 7 shows the curing characteristics of the rubber composites. Rubber composites should have suitable scorch time (T_{c10}) and optimal curing time (T_{c90}) to meet processing performance requirements [51]. The minimum torque (M_L) characterizes the degree of interaction between filler particles. The smaller the value, the weaker the interactions between the filler, and the better the dispersion of the filler in the matrix [45]. The maximum torque (M_H) reflects the degree of interactions between the filler and matrix [52], and the torque difference (M_H-M_L) value is positively correlated with the extent of crosslinking of the rubber compound [45]. It can be seen from Figure 7a that the addition of EEUG caused the T_{c10} of the rubber compound to fluctuate slightly. This is because the internal epoxy group of the EEUG in the rubber compound opened and crosslinked under the action of heat or a coupling agent, thereby affecting the T_{c10} [53,54]. Both MTES-modified SiO_2 and the addition of EEUG reduced the T_{c90} and M_L of the compound, while the maximum torque (M_H) and the torque difference (M_H-M_L) increased. This shows that the modified SiO_2 had better dispersion and a higher degree of interaction with the matrix, and its composite had a higher crosslinking density. Analysis suggests that both the small-molecule coupling agent MTES and the macromolecular modifier EEUG bonded with the silanol groups on the surface of SiO_2, thereby reducing the number of silanol groups on its surface. This decreased its surface polarity, weakened its agglomeration tendency, enhanced the dispersion of SiO_2, and further reduced its adsorption of vulcanization accelerators, thereby reducing the vulcanization time [51,55,56]. Modified SiO_2 had a weaker aggregation tendency, could be better dispersed in the rubber matrix, had a higher degree of interaction with the rubber matrix, and increased the crosslinking density.

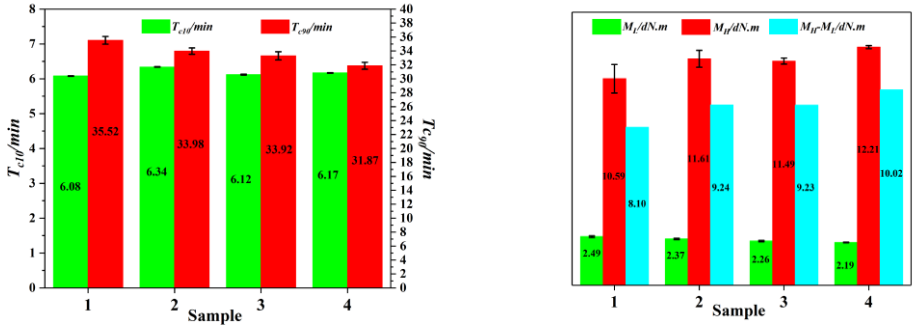

(**a**) (**b**)

Figure 7. The curing characteristics of rubber: (**a**) The scorch time (T_{c10}) and curing time (T_{c90}); (**b**) The minimum torque (M_L), maximum torque (M_H) and torque difference (M_H-M_L); (1) SiO_2/EUG/SBR; (2) MEST-SiO_2/EUG/SBR; (3) SiO_2/EEUG/EUG/SBR; (4) MTES-SiO_2/EEUG/EUG/SBR.

3.6. Rubber Processing Analyzer of Rubber Composites

The RPA results of rubber composites are shown in Figure 8. Generally, the storage modulus (G') is used to indicate the degree of interaction between fillers inside rubber compounds. The phenomenon that G' decreases with the increase in strain is called the Payne effect [35]. When G' is large, the fillers strongly interact with each other, and the Payne effect is more obvious. It can be seen from Figure 8a that compared with the composite with unmodified SiO_2, both MTES-modified SiO_2 and the addition of EEUG significantly reduced the G' of the composite at low strain, while there was not a significant difference in the high-strain region. The composite with both EEUG and MTES-SiO_2 added displayed the best filler dispersion, and its G' at low strain was the smallest, indicating the least interactions between fillers. This is because MTES reacts with the silanol groups on the surface of SiO_2, reducing interactions between SiO_2. At the same time, EEUG forms hydrogen bonds or covalent bonds with the silanol groups on the surface of SiO_2, which

further reduces the interactions between SiO_2 [57]. It can be seen from Figure 8b that the loss factor (*tanδ*) of MTES-modified SiO_2 and EEUG-added composites were both significantly lower at low strain compared with the composites with unmodified SiO_2. The synergy of EEUG and MTES makes SiO_2 produce the best dispersion and compatibility with the rubber matrix. Well-dispersed fillers further limit the mobility of the matrix molecular segments, and the abrasion between fillers and the internal friction loss of the rubber matrix molecular segments can be reduced [8,38]. Therefore, the MTES-SiO_2/EEUG/EUG/SBR composite had the lowest loss factor.

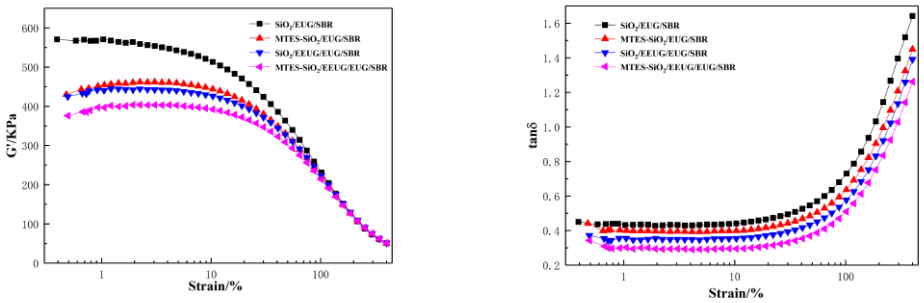

(**a**) (**b**)

Figure 8. Rubber processing analyzer (RPA) curves of rubber composites: (**a**) G'–strain curve; (**b**) *tanδ*–strain curve.

3.7. Mechanical Performance of Rubber Composites

Figure 9a shows the stress–strain curves of the rubber composites, and Figure 9b–d shows the mechanical properties of the rubber composites. It can be seen from Figure 9a that both MTES-modified SiO_2 and the addition of EEUG increased the modulus of the composite. The composite with both EEUG and MTES-SiO_2 added had the highest modulus, which was attributed to the good dispersion of SiO_2 in the matrix. It can be seen from Figure 9b–d that both MTES-modified SiO_2 and the addition of EEUG improved the tensile strength, modulus at 100% strain, modulus at 300% strain, and tear strength of the rubber composite. The Shore hardness of the rubber composite material was basically unchanged, while still maintaining good elongation at break. The good dispersion of SiO_2 and its compatibility with the matrix endowed the composite with excellent comprehensive properties. Compared with the composite with unmodified SiO_2, the tensile strength of the composite with both EEUG and MTES-SiO_2 added increased by 42.1%, the modulus at 100% strain increased by 88.5%, the modulus at 300% strain increased by 130.8%, and the tear strength increased by 39.9%.

3.8. Wear Resistance and Wet Skid Resistance of Rubber Composites

Figure 10a shows the Akron abrasion and density of rubber composites. The MTES-modified SiO_2 and the addition of EEUG had little effect on the density of the composite, but it significantly reduced the Akron wear of the material and improved the wear resistance. Compared with the composite with unmodified SiO_2, the abrasion volume of the composite with both EEUG and MTES-SiO_2 added was reduced by 50.9%, and the wear resistance was significantly improved. According to the analysis, in the compound with unmodified SiO_2, the compatibility of the filler and the matrix was not good, and the large agglomerated particles easily separated from the matrix. The resulting cavity became a weak point of the compound. Upon further deformation of the rubber, these weak points formed cracks on the surface or inside the rubber, causing the wear volume to increase [58,59]. The synergy of EEUG and MTES allows SiO_2 to be well-dispersed and compatible with the matrix. This limited the movement of the material's molecular chain when external forces were applied, and improved the material's ability to resist friction. At the same time, the good compatibility of SiO_2 and the matrix increased the bonding strength between the filler

and the matrix. This prevented it from being easily damaged during the friction process, so the abrasion volume was reduced [54]. Moreover, the better the dispersion of SiO_2 particles, the more difficult the path of crack propagation, the smoother the path of stress transmission to the SiO_2 particles, and the less likely the composite will form cracks on its surface [59,60]. This effectively improved the wear resistance of the composite.

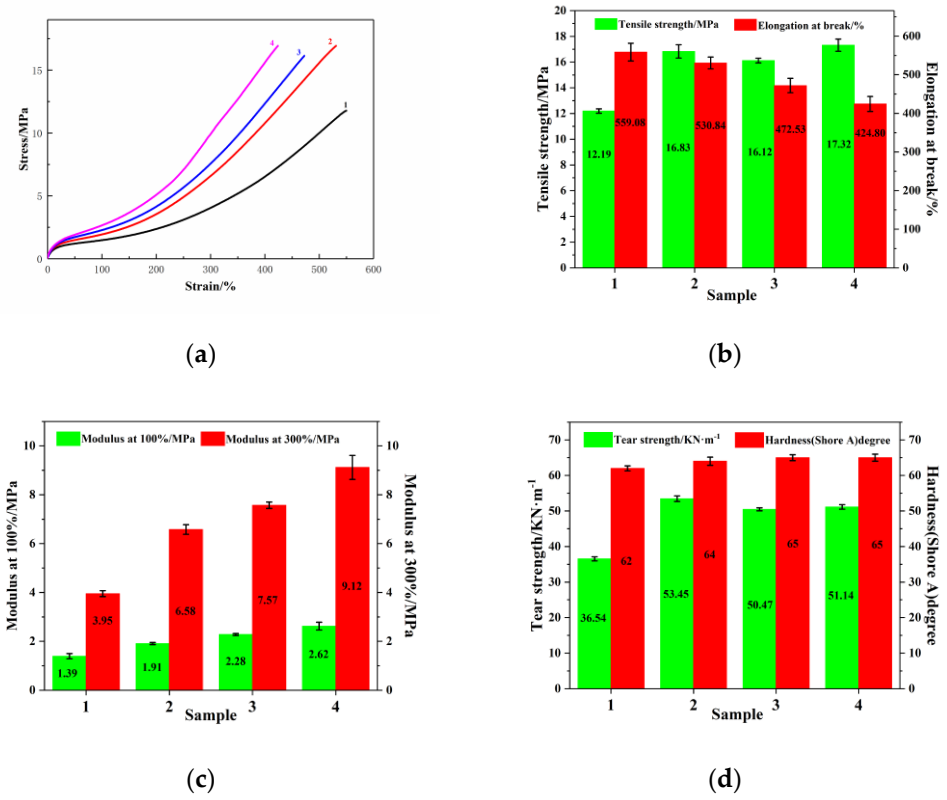

Figure 9. (**a**) The stress–strain curves of rubber composites. (**b**–**d**) The mechanical properties of the rubber composites. (1) SiO_2/EUG/SBR, (2) MEST-SiO_2/EUG/SBR, (3) SiO_2/EEUG/EUG/SBR, (4) MTES-SiO_2/EEUG/EUG/SBR.

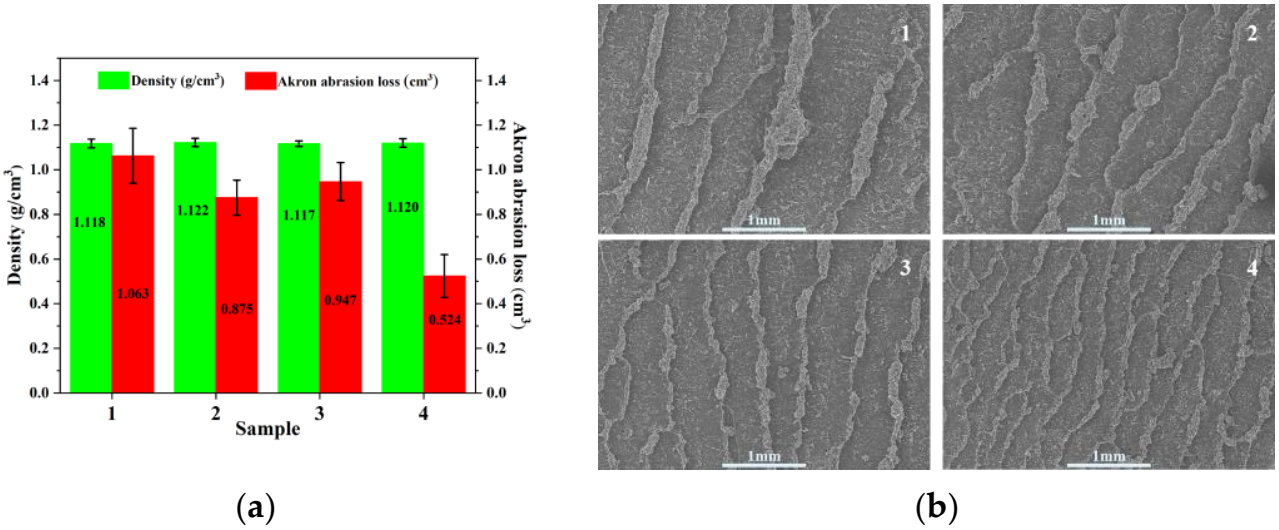

Figure 10. (**a**) The Akron abrasion and density of rubber composites; (**b**) SEM of the wear surface morphology of the rubber composite. (1) SiO_2/EUG/SBR; (2) MEST-SiO_2/EUG/SBR; (3) SiO_2/EEUG/EUG/SBR; (4) MTES-SiO_2/EEUG/EUG/SBR.

Figure 10b shows a SEM image of the wear surface morphology of the rubber composite. The composite with unmodified SiO_2 had high and wide ridges on its wear surface, and the distance between the ridges was relatively large. The ridges produced on the surface of the MTES-modified SiO_2 and EEUG-added composite became shorter and narrower, and the distance between the ridges became smaller. This indicates that the wear resistance of the material was improved. The composite with both EEUG and MTES-SiO_2 added had the shortest and narrowest ridges, and the distance between ridges was the smallest, indicating that it had the strongest resistance to friction and the best wear resistance.

Figure 11 shows the wet friction coefficient of the rubber composites. The MTES-modified SiO_2 and the addition of EEUG increased the wet friction coefficient of the composite material. Compared with the composite with unmodified SiO_2, the wet friction coefficient of the composite with both EEUG and MTES-SiO_2 added increased by 43.2%. Analysis showed that SiO_2 helped pierce the water film on the rubber surface and reduced the thickness of the water film, so the rubber could contact the ground faster, increased the contact area between the rubber and the ground, and achieved an anti-skid effect [9]. The dispersion of SiO_2 in the MTES-SiO_2/EEUG/EUG/SBR composite and its compatibility with the matrix were the best, which prevented it from separating from the matrix, the wet friction coefficient of the rubber composite was significantly improved, thereby improving the wet skid resistance of the rubber compound. This can help shorten the braking distance on wet roads and improve the safety factor of tires.

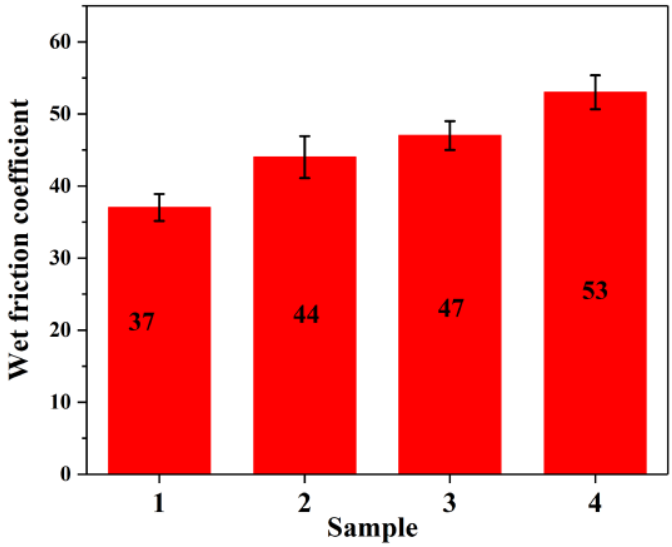

Figure 11. The wet friction coefficient of rubber composites. (1) SiO_2/EUG/SBR; (2) MEST-SiO_2/EUG/SBR; (3) SiO_2/EEUG/EUG/SBR; (4) MTES-SiO_2/EEUG/EUG/SBR.

4. Conclusions

The synergistic effect of a small molecule coupling agent and macromolecular modifier significantly improved the dispersion of SiO_2 in the rubber matrix and the interfacial compatibility with the matrix. The MTES reacted with the silanol groups on the surface of SiO_2 to form a covalent bond, which reduced the surface activity and agglomeration tendency of SiO_2. The epoxy group on the EEUG can form hydrogen bonds or covalent bonds with the silanol groups on the surface of SiO_2, which anchors part of the SiO_2 to the EEUG molecular chain. During processing, the shear flow of EEUG molecular chains can drive better dispersion of SiO_2 in the rubber matrix. The results verified that compared to the composite with added unmodified SiO_2, the composite with both EEUG and MTES-SiO_2 added had higher binder content, better filler dispersion, better wear resistance, and wet skid resistance. Thus, this work exhibited great potential in the rubber and tire industry.

Author Contributions: Methodology, M.L.; Formal analysis, M.L. and K.W.; Investigation, M.L., K.W. and Y.X.; Data curation, M.L. and K.W.; Writing—original draft preparation, M.L., K.W. and Y.X.; Writing—review and editing, Y.X.; Supervision, Y.X.; Funding acquisition, Y.X. All authors have read and agreed to the published version of the manuscript.

Funding: This research was funded by the National Natural Science Foundation of China (NSFC No. 52063006); the Science and Technology Foundation of Guizhou Province (Grant No. [2019]2166); and the Science and Technology Foundation of Guizhou Province (grant number 2019-112-016).

Data Availability Statement: Data are contained within this article.

Conflicts of Interest: The authors declare no conflict of interest.

References

1. Waddell, W.H.; Evans, L.R. Use of nonblack fillers in tire compounds. *Rubber Chem. Technol.* **1996**, *69*, 377–423. [CrossRef]
2. Rattanasom, N.; Saowapark, T.; Deeprasertkul, C. Reinforcement of natural rubber with silica/carbon black hybrid filler. *Polym. Test.* **2007**, *26*, 369–377. [CrossRef]
3. Tse, M.F. BIMS/filler interactions. I. Effects of filler structure. *J. Appl. Polym. Sci.* **2006**, *100*, 4943–4956. [CrossRef]
4. Hilonga, A.; Kim, J.K.; Sarawade, P.B.; Quang, D.V.; Shao, G.N.; Elineema, G.; Kim, H.T. Synthesis of mesoporous silica with superior properties suitable for green tire. *J. Ind. Eng. Chem.* **2012**, *18*, 1841–1844. [CrossRef]
5. Li, Y.; Han, B.; Wen, S.; Lu, Y.; Yang, H.; Zhang, L.; Liu, L. Effect of the temperature on surface modification of silica and properties of modified silica filled rubber composites. *Compos. Part. A Appl. Sci. Manuf.* **2014**, *62*, 52–59. [CrossRef]
6. Pan, X.D. Impact of reinforcing filler on the dynamic moduli of elastomer compounds under shear deformation in relation to wet sliding friction. *Rheol. Acta* **2005**, *44*, 379–395. [CrossRef]
7. Gal, L.A.; Yang, X.; Klüppel, M. Evaluation of sliding friction and contact mechanics of elastomers based on dynamic-mechanical analysis. *J. Chem. Phys.* **2005**, *123*, 014704. [CrossRef]
8. Gao, W.; Lu, J.; Song, W.; Hu, J.; Han, B. Interfacial interaction modes construction of various functional SSBR–silica towards high filler dispersion and excellent composites performances. *RSC Adv.* **2019**, *9*, 18888–18897. [CrossRef]
9. Wang, Y.X.; Wu, Y.P.; Li, W.J.; Zhang, L.Q. Influence of filler type on wet skid resistance of SSBR/BR composites: Effects from roughness and micro-hardness of rubber surface. *Appl. Surf. Sci.* **2011**, *257*, 2058–2065. [CrossRef]
10. Palraj, S.; Selvaraj, M.; Maruthan, K.; Rajagopal, G. Corrosion and wear resistance behavior of nano-silica epoxy composite coatings. *Prog. Org. Coat.* **2015**, *81*, 132–139. [CrossRef]
11. Peng, Z.; Kong, L.X.; Li, S.D.; Chen, Y.; Huang, M.F. Self-assembled natural rubber/silica nanocomposites: Its preparation and characterization. *Compos. Sci. Technol.* **2007**, *67*, 3130–3139. [CrossRef]
12. Mizutani, T.; Arai, K.; Miyamoto, M.; Kimura, Y. Application of silica-containing nano-composite emulsion to wall paint: A new environmentally safe paint of high performance. *Prog. Org. Coat.* **2006**, *55*, 276–283. [CrossRef]
13. Doan, V.A.; Nobukawa, S.; Ohtsubo, S.; Tada, T.; Yamaguchi, M. Selective migration of silica particles between rubbers. *J. Polym. Res.* **2013**, *20*, 1–6. [CrossRef]
14. Reuvekamp, L.A.; Ten Brinke, J.W.; Van Swaaij, P.J.; Noordermeer, J.W. Effects of time and temperature on the reaction of TESPT silane coupling agent during mixing with silica filler and tire rubber. *Rubber Chem. Technol.* **2002**, *75*, 187–198. [CrossRef]
15. Qu, L.; Yu, G.; Wang, L.; Li, C.; Zhao, Q.; Li, J. Effect of filler–elastomer interactions on the mechanical and nonlinear viscoelastic behaviors of chemically modified silica-reinforced solution-polymerized styrene butadiene rubber. *J. Polym. Sci.* **2012**, *126*, 116–126. [CrossRef]
16. Venter, S.A.S.; Kunita, M.H.; Matos, R.; Nery, R.C.; Radovanovic, E.; Muniz, E.C.; Girotto, E.M.; Rubira, A.F. Thermal and scanning electron microscopy/energy-dispersive spectroscopy analysis of styrene–butadiene rubber–butadiene rubber/silicon dioxide and styrene–butadiene rubber–butadiene rubber/carbon black–silicon dioxide composites. *J. Appl. Polym. Sci.* **2005**, *96*, 2273–2279. [CrossRef]
17. Prasertsri, S.; Rattanasom, N. Mechanical and damping properties of silica/natural rubber composites prepared from latex system. *Polym. Test.* **2011**, *30*, 515–526. [CrossRef]
18. Katueangngan, K.; Tulyapitak, T.; Saetung, A.; Soontaranon, S.; Nithi-uthai, N. Renewable interfacial modifier for silica filled natural rubber compound. *Procedia Chem.* **2016**, *19*, 447–454. [CrossRef]
19. Mohapatra, S.; Alex, R.; Nando, G.B. Cardanol grafted natural rubber: A green substitute to natural rubber for enhancing silica filler dispersion. *J. Appl. Polym. Sci.* **2016**, *133*, 43057. [CrossRef]
20. Lopez, J.F.; Perez, L.D.; Lopez, B.L. Effect of silica modification on the chemical interactions in NBR-based composites. *J. Appl. Polym. Sci.* **2011**, *122*, 2130–2138. [CrossRef]
21. Wang, M.; Morris, M.D.; Kutsovsky, Y. Effect of fumed silica surface area on silicone rubber reinforcement. *KGK-Kaut. Gummi Kunst.* **2008**, *61*, 107.
22. Kaewsakul, W.; Sahakaro, K.; Dierkes, W.K.; Noordermeer, J.W. Optimization of mixing conditions for silica-reinforced natural rubber tire tread compounds. *Rubber Chem. Technol.* **2012**, *85*, 277–294. [CrossRef]

23. Liu, X.; Zhao, S.; Zhang, X.; Li, X.; Bai, Y. Preparation, structure, and properties of solution-polymerized styrene-butadiene rubber with functionalized end-groups and its silica-filled composites. *Polymer* **2014**, *55*, 1964–1976. [CrossRef]
24. Liu, X.; Zhao, S.; Yang, Y.; Zhang, X.; Wu, Y. Structure and properties of star-shaped solution-polymerized styrene-butadiene rubber and its co-coagulated rubber filled with silica/carbon black-I: Morphological structure and mechanical properties. *Polym. Advan. Technol.* **2009**, *20*, 818–825. [CrossRef]
25. Wang, M.J. Effect of polymer-filler and filler-filler interactions on dynamic properties of filled vulcanizates. *Rubber Chem. Technol.* **1998**, *71*, 520–589. [CrossRef]
26. Sun, Z.; Huang, Q.; Zhang, L.; Wang, Y.; Wu, Y. Tailoring silica-rubber interactions by interface modifiers with multiple functional groups. *RSC Adv.* **2017**, *7*, 38915–38922. [CrossRef]
27. Hashim, A.S.; Azahari, B.; Ikeda, Y.; Kohjiya, S. The effect of bis (3-triethoxysilylpropyl) tetrasulfide on silica reinforcement of styrene-butadiene rubber. *Rubber Chem. Technol.* **1998**, *71*, 289–299. [CrossRef]
28. Lee, S.Y.; Kim, J.S.; Lim, S.H.; Jang, S.H.; Kim, D.H.; Park, N.H.; Jung, J.W.; Choi, J. The investigation of the silica-reinforced rubber polymers with the methoxy type silane coupling agents. *Polymers* **2020**, *12*, 3058. [CrossRef] [PubMed]
29. Wu, C.L.; Zhang, M.Q.; Rong, M.Z.; Friedrich, K. Silica nanoparticles filled polypropylene: Effects of particle surface treatment, matrix ductility and particle species on mechanical performance of the composites. *Compos. Sci. Technol.* **2005**, *65*, 635–645. [CrossRef]
30. Kapgate, B.P.; Das, C.; Basu, D.; Das, A.; Heinrich, G. Rubber composites based on silane-treated stöber silica and nitrile rubber: Interaction of treated silica with rubber matrix. *J. Elastom. Plast.* **2015**, *47*, 248–261. [CrossRef]
31. Bertora, A.; Castellano, M.; Marsano, E.; Alessi, M.; Conzatti, L.; Stagnaro, P.; Colucci, G.; Priola, A.; Turturro, A. A new modifier for silica in reinforcing SBR elastomers for the tyre industry. *Macromol. Mater. Eng.* **2011**, *296*, 455–464. [CrossRef]
32. Dong, H.; Luo, Y.; Lin, J.; Bai, J.; Chen, Y.; Zhong, B.; Jia, D. Effects of modified silica on the co-vulcanization kinetics and mechanical performances of natural rubber/styrene–butadiene rubber blends. *J. Appl. Polym. Sci.* **2020**, *137*, 48838. [CrossRef]
33. Li, Y.; Han, B.; Liu, L.; Zhang, F.; Zhang, L.; Wen, S.; Lu, Y.; Yang, H.; Shen, J. Surface modification of silica by two-step method and properties of Solution Styrene Butadiene Rubber (SSBR) nanocomposites filled with modified silica. *Compos. Sci. Technol.* **2013**, *88*, 69–75. [CrossRef]
34. Sarkawi, S.S.; Dierkes, W.K.; Noordermeer, J.W. Elucidation of filler-to-filler and filler-to-rubber interactions in silica-reinforced natural rubber by TEM Network Visualization. *Eur. Polym. J.* **2014**, *54*, 118–127. [CrossRef]
35. Sengloyluan, K.; Sahakaro, K.; Dierkes, W.K.; Noordermeer, J.W. Silica-reinforced tire tread compounds compatibilized by using epoxidized natural rubber. *Eur. Polym. J.* **2014**, *51*, 69–79. [CrossRef]
36. Xu, T.; Jia, Z.; Luo, Y.; Jia, D.; Peng, Z. Interfacial interaction between the epoxidized natural rubber and silica in natural rubber/silica composites. *Appl. Surf. Sci.* **2015**, *328*, 306–313. [CrossRef]
37. Xia, L.; Wang, Y.; Ma, Z.; Du, A.; Qiu, G.; Xin, Z. Preparation of epoxidized Eucommia ulmoides gum and its application in Styrene-Butadiene Rubber (SBR)/silica composites. *Polym. Adv. Technol.* **2017**, *28*, 94–101. [CrossRef]
38. Wang, Y.; Liu, J.; Xia, L.; Shen, M.; Xin, Z.; Kim, J. Role of epoxidized natural Eucommia ulmoides gum in modifying the interface of styrene-butadiene rubber/silica composites. *Polym. Adv. Technol.* **2019**, *30*, 2968–2976. [CrossRef]
39. Yang, J.; Chen, J. Surface free energies and steam stability of methyl-modified silica membranes. *J. Porous. Mat.* **2009**, *16*, 737. [CrossRef]
40. Jiang, H.; Zheng, Z.; Wang, X. Kinetic study of methyltriethoxysilane (MTES) hydrolysis by FTIR spectroscopy under different temperatures and solvents. *Vib. Spectrosc.* **2008**, *46*, 1–7. [CrossRef]
41. Xiong, W.; Yang, D.; Yang, R.; Li, Y.; Zhou, H.; Qiu, X. Preparation of lignin-based silica composite submicron particles from alkali lignin and sodium silicate in aqueous solution using a direct precipitation method. *Ind. Crop. Prod.* **2015**, *74*, 285–292. [CrossRef]
42. Cao, F.; Kim, D.; Li, X.; Feng, C.; Song, Y. Synthesis of polyaluminocarbosilane and reaction mechanism study. *J. Appl. Polym. Sci.* **2002**, *85*, 2787–2792. [CrossRef]
43. Xu, T.; Jia, Z.; Wu, L.; Chen, Y.; Luo, Y.; Jia, D.; Peng, Z. Influence of acetone extract from natural rubber on the structure and interface interaction in NR/silica composites. *Appl. Surf. Sci.* **2017**, *423*, 43–52. [CrossRef]
44. Xu, C.; Xu, G.; Du, M.; Zhu, H.; Fu, Y.; Zhang, X. Effects of plant polyphenols on the interface and mechanical properties of rubber/silica composites. *Polym. Polym. Compos.* **2012**, *20*, 853–860. [CrossRef]
45. Sun, D.; Li, X.; Zhang, Y.; Li, Y. Effect of modified nano-silica on the reinforcement of styrene butadiene rubber composites. *J. Macromol. Sci. Part B* **2011**, *50*, 1810–1821. [CrossRef]
46. Bernal-Ortega, P.; Anyszka, R.; Morishita, Y.; Ronza, D.R.; Blume, A. Comparison between SBR compounds filled with in-situ and ex-situ silanized silica. *Polymers* **2021**, *13*, 281. [CrossRef]
47. Sengloyluan, K.; Sahakaro, K.; Dierkes, W.K.; Noordermeer, J.W. Reduced ethanol emissions by a combination of epoxidized natural rubber and silane coupling agent for silica-reinforced natural rubber-based tire treads. *Rubber Chem. Technol.* **2016**, *89*, 419–435. [CrossRef]
48. Choi, S.S. Influence of storage time and temperature and silane coupling agent on bound rubber formation in filled styrene–butadiene rubber compounds. *Polym. Test.* **2002**, *21*, 201–208. [CrossRef]
49. Bach, Q.V.; Vu, C.M.; Vu, H.T. Effects of co-silanized silica on the mechanical properties and thermal characteristics of natural rubber/styrene-butadiene rubber blend. *Silicon* **2020**, *12*, 1799–1809. [CrossRef]

50. Sarkawi, S.S.; Aziz, A.K.C.; Rahim, R.A.; Ghani, R.A.; Kamaruddin, A.N. Properties of epoxidized natural rubber tread compound: The hybrid reinforcing effect of silica and silane system. *Polym. Polym. Compos.* **2016**, *24*, 775–782. [CrossRef]
51. Zhao, Z.; Zhao, X.; Gong, G.; Zheng, J.; Liang, T.; Yin, C.; Zhang, Q. Influence of particle type and silane coupling agent on properties of particle-reinforced styrene-butadiene rubber. *Polym-Plast. Technol.* **2012**, *51*, 268–272. [CrossRef]
52. Yin, C.; Zhang, Q.; Gu, J.; Zhao, Z.; Zheng, J.; Gong, G.; Liang, T.; Zhang, H. Cure characteristics and mechanical properties of vinyltriethoxysilane grafted styrene-butadiene rubber/silica blends. *Polym-Plast. Technol.* **2012**, *51*, 1218–1222. [CrossRef]
53. Manna, A.K.; De, P.P.; Tripathy, D.K.; De, S.K.; Peiffer, D.G. Bonding between precipitated silica and epoxidized natural rubber in the presence of silane coupling agent. *J. Appl. Polym. Sci.* **1999**, *74*, 389–398. [CrossRef]
54. Mensah, B.; Agyei-Tuffour, B.; Nyankson, E.; Bensah, Y.D.; Dodoo-Arhin, D.; Bediako, J.K.; Onwona-Agyeman, B.; Yaya, A. Preparation and characterization of rubber blends for industrial tire tread fabrication. *Int. J. Polym. Sci.* **2018**, *2018*, 2473286. [CrossRef]
55. Chen, L.; Jia, Z.; Tang, Y.; Wu, L.; Luo, Y.; Jia, D. Novel functional silica nanoparticles for rubber vulcanization and reinforcement. *Compos. Sci. Technol.* **2017**, *144*, 11–17. [CrossRef]
56. George, K.M.; Varkey, J.K.; Thomas, K.T.; Mathew, N.M. Epoxidized natural rubber as a reinforcement modifier for silica-filled nitrile rubber. *J. Appl. Polym. Sci.* **2002**, *85*, 292–306. [CrossRef]
57. Sengloyluan, K.; Sahakaro, K.; Noordermeer, J.W. Silica-reinforced natural rubber compounds compatibilized through the use of epoxide functional groups and tespt combination. *Adv. Mat. Res.* **2013**, *844*, 272–275. [CrossRef]
58. Singh, V.K.; Gope, P.C. Silica-styrene-butadiene rubber filled hybrid composites: Experimental characterization and modeling. *J. Reinf. Plast. Comp.* **2010**, *29*, 2450–2468. [CrossRef]
59. Martin, P.J.; Brown, P.; Chapman, A.V.; Cook, S. Silica-reinforced epoxidized natural rubber tire treads-performance and durability. *Rubber Chem. Technol.* **2015**, *88*, 390–411. [CrossRef]
60. Seo, G.; Park, S.M.; Ha, K.; Choi, K.T.; Hong, C.K.; Kaang, S. Effectively reinforcing roles of the networked silica prepared using 3, 3′-bis (triethoxysilylpropyl) tetrasulfide in the physical properties of SBR compounds. *J. Mater. Sci.* **2010**, *45*, 1897–1903. [CrossRef]